AD-A071 735 CORNELL UNIV ITHACA N Y SCHOOL OF ELECTRICAL ENGINEERING F/G 20/12
A STUDY OF ALLOY SCATTERING IN GA1-XALXAS,(U)
JUN 79 A CHANDRA, L F EASTMAN N00014-75-C-0739

UNCLASSIFIED NL

1 OF 1
AD
A071735

END
DATE
FILMED
8-79
DDC

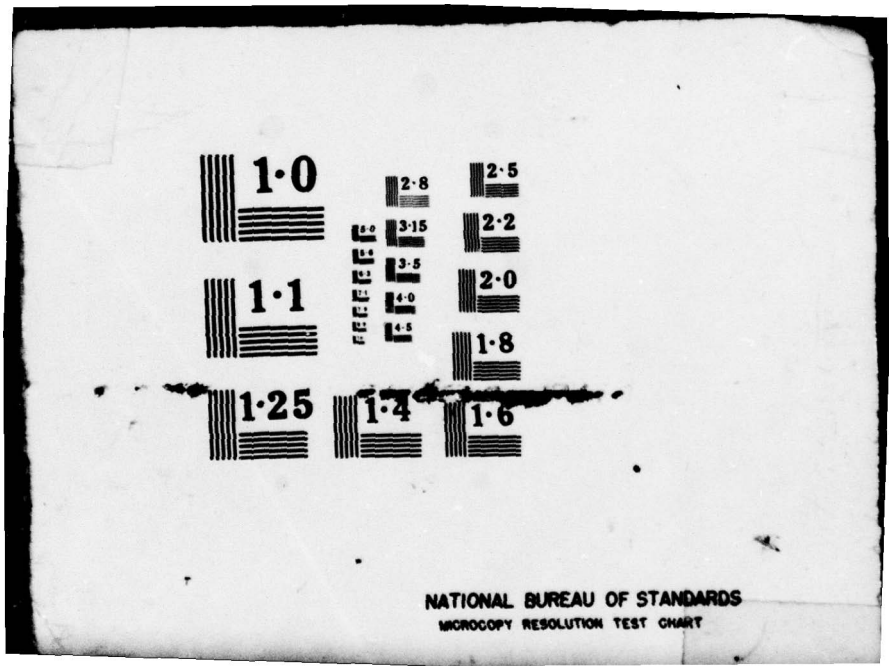
1·0
1·1
1·25
2·8
3·15
3·5
4·0
4·5
1·4
2·5
2·2
2·0
1·8
1·6
NATIONAL BUREAU OF STANDARDS
MICROCOPY RESOLUTION TEST CHART

AD A071735

A STUDY OF ALLOY SCATTERING IN $Ga_{1-x}Al_xAs$

by

Amitabh Chandra & Lester F. Eastman
~~School of Electrical Engineering~~
~~Cornell University~~
~~Ithaca, N.Y. 14853~~

22 Jun 79

N00014-75-C-0739
Date: 22 June 1979

N00014-75-C-0739

31 pp

ABSTRACT

The temperature dependence of electron mobility of high purity ($n < 1 \times 10^{15}$ cm^{-3}) LPE $Ga_{1-x}Al_xAs$ layers ($x < .18$) has been studied in the range 25°K - 110°K to measure the extents of alloy-like and ionized impurity scattering. Values of the alloy scattering parameter ΔE (which may include a contribution from space charge scattering) determined for these samples were found to lie in the range .36 eV to .51 eV, the average being .44 eV. The compensation ratio was found to be about 2, and independent of x.

Delta

10 to the 15th power/cc

I. INTRODUCTION

A. Alloy Scattering

Alloy scattering of electrons in a semiconductor alloy such as $Ga_{1-x}Al_xAs$ is caused by randomness in the distribution of the alloying constituents. An expression for the alloy scattering component of mobility μ_A was first derived by Brooks[1,2] as

$$\mu_A = \frac{(2\pi)^{\frac{1}{2}}}{3} \frac{q \hbar^4 N_a}{(kT)^{\frac{1}{2}} m^{*\frac{5}{2}} x(1-x)(\Delta E)^2} \qquad (1)$$

where q is the electronic charge, $\hbar$ is (Plank's constant)/2π, N_a is the density of alloying sites, k is Boltzmann's constant, T is the absolute temperature, m* is the effective electron mass, x and (1-x) are the mole fractions of the binary end compounds, and ΔE is an energy step which was assumed equal to the band-gap difference between the end compounds.

In a recent paper,[3] Harrison and Hauser derived a similar expression for alloy scattering. They assumed the crystal to have a uniform background potential with square wells of depth ΔE at random sites associated with one of the alloying constituents. The square well potential was assumed to extend over a spherical region of radius equal to the nearest neighbour separation, a choice they admitted as being somewhat arbitrary. They obtained the

energy dependent scattering time $\tau_A(\varepsilon)$ as

$$\tau_A(\varepsilon) = \frac{8}{3\sqrt{2}\pi} \frac{\hbar^4 N_a \varepsilon^{-\frac{1}{2}}}{(kT)^{\frac{1}{2}} m^{*\frac{3}{2}} x(1-x)(\Delta E)^2} \qquad (2)$$

where $\varepsilon = (E-E_c)/kT$ is the electronic kinetic energy normalized to kT. Multiplying Eq. (2) by $\frac{4}{3\sqrt{\pi}} \frac{q}{m^*}$ gives an expression for μ_A that is identical to Brooks' expression except for a constant factor. Thus, for a given set of physical parameters, $(\mu_A)_{Brk} = 1.85\ (\mu_A)_{HH}$, where Brk and HH denote the use of expressions (1) and (2) respectively to calculate μ_A.

In Brooks' original formulation, ΔE was taken to be the band gap difference between the two end compounds.[4] For ternary alloys where both end compounds have direct gaps, (such as $Ga_{1-x}In_xAs$), there is no ambiguity. However, if one of the end compounds is direct and the other is indirect, as in $Ga_{1-x}Al_xAs$, then the question arises whether ΔE is the band gap difference ($\Delta E_g = 0.73$ eV) or the <u>direct</u> band gap difference ($\Delta(E_{\Gamma c}-E_{\Gamma v}) = 1.52$ eV). Harrison and Hauser[3] have suggested that instead of ΔE_g, ΔE should be taken as the conduction band edge discontinuity ΔE_c between the end compounds. Again, taking ΔE to be $\Delta(E_c - E_{vac})$ gives a value 0.55 eV, while $\Delta(E_{\Gamma c} - E_{vac})$ gives 1.34 eV. Finally, Ferry[5] has used the

electronegativity differences to predict that ΔE for $Ga_{1-x}Al_xAs$ should be .12 eV at x = .5.

It is clear that depending on which of the several "justifiable" values of ΔE (ranging from .12 eV to 1.52 eV) is selected, and which of the two expressions (1) and (2) is used, alloy scattering in $Ga_{1-x}Al_xAs$ can be represented as being negligible, moderate, or dominant. Thus until a clearer theory of alloy scattering is developed, we must turn to experiment to determine the value of ΔE.

B. Space Charge Scattering

Space charge scattering in semiconductors is caused by space charge regions that form around localized composition and impurity concentration inhomogeneities. This mechanism was first discussed by Weisberg[6] to explain anamolously low mobilities in GaAs. Later, Conwell and Vassel[7] proposed a simple model where the space charge scattering time was given by

$$\tau_{sc}(\varepsilon) = (NsQv)^{-1} \qquad (3)$$

from which the space charge mobility component is obtained as

$$\mu_{SC} = 2.4\times10^{9}/(m^*/m_o)^{\frac{1}{2}}\, T^{\frac{1}{2}}\, NsQ \quad cm^2/Vsec \qquad (4)$$

where Ns is the volume density (cm^{-3}) of the space charge scattering centers and can vary widely depending on the

quality of the sample, Q is the cross sectional area of the centers (cm^2) and v is the electron velocity (cm/sec).

Subsequently Katoda et al [8] and others[9,10] have used Eqs. (3) and (4), which have the same temperature and energy dependence as alloy scattering, to describe space charge scattering. However Weisberg[6] obtained the temperature dependence of the scattering cross section Q to be $(n/T)^{1/3}$, so that

$$\mu_{SC} \sim n^{\frac{1}{3}} T^{-\frac{5}{6}} , \qquad (5)$$

n being the free carrier density.

We are inclined a priori to agree with Eq. (5). However, in this work we found it necessary to ignore the $(n/T)^{\frac{1}{3}}$ dependence of Q. Since we were attempting to measure the extent of alloy scattering experimentally, merging space charge scattering with alloy scattering would simplify our analysis considerably. Furthermore, our results showed that space charge scattering does not dominate over alloy scattering in our high pruity samples, as it does in samples studied by Kaneko et al.[9] and Stringfellow.[10] This offered a post-priori justification for making this approximation.

We use the term "alloy-like" scattering to collectively denote the scattering mechanisms with the $(\varepsilon T)^{-\frac{1}{2}}$ relaxation time dependence. We define the "alloy-like" scattering parameter, E_B, of a given ternary sample to be the

value of ΔE in Eq. (2) required to fit the experimental μ vs T data, when ionized impurity and lattice scattering is also considered. Thus defined, E_B absorbs any arbitrariness in the constant factor in Eq. (2), and includes contributions (if any) from space charge scattering. Our choice of Eq. (2) over Eq. (1) in defining E_B rests entirely on the fact that the derivation of the latter is unpublished. Using Eq. (1) instead of Eq. (2) to define E_B would give values higher by a factor 1.36.

In this study we report on the experimental determination of E_B for nine samples of high purity $Ga_{1-x}Al_xAs$ ($x < .18$) grown by LPE.

II. EXPERIMENT

A. Principle of the Experiment

The alloy scattering parameter E_B can be determined experimentally by separating the various scattering mechanisms in $Ga_{1-x}Al_xAs$. The Hall mobility μ_H of a ternary alloy is a function of x, T, B, N_S and E_B, where B is the magnetic field and $N_S = (N_D^+ + N_A)$ times the screening factor. By estimating the various physical parameters, for a given x and T (as described in section III-B) the polar optical, deformation potential and piezoelectric scattering time constants can be determined. The ionized impurity scattering relaxation time τ_{II} can be determined

as a function of N_S, while alloy scattering can be expressed in terms of E_B, both of which are unknown. Thus the net relaxation time, the drift mobility, and the Hall mobility of $Ga_{1-x}Al_xAs$ can be calculated as functions of N_S and E_B, as described in section III-C.

To measure N_S and E_B, use is made of the fact that τ_{II} varies as $T^{3/2}$ while τ_A varies as $T^{-1/2}$. By measuring μ_H over a temperature range, the alloy and the ionized impurity components can be separated from the residual scattering (i.e., after phonon scattering has been subtracted from the total).

B. Experiment

The Hall mobility measurements were made on ten layers of high purity n $Ga_{1-x}Al_xAs$ ($x < .18$) (and one reference layer of undoped n GaAs), grown by LPE at 700 - 680°C.[11] The layers were 9-14 microns thick and were grown on nonconverting S.I. GaAs substrates. Two layers were grown from each of five Ga-Al-As melts of increasing Al concentration. The first layers will be referred to at type-A, and the second as type-B layers. Van der Pauw Hall samples were fabricated from each layer, and tin dot contacts were alloyed under hydrogen using a strip heater. Good ohmic contacts were obtained. Van der Pauw measurements were made on samples at B = 2 KGauss, at 5° intervals from 25°K to 110°K.

The Hall mobility μ_H and the Hall carrier density per unit area Q_H obtained from the measurements are plotted against temperature in Figs. 1 and 2 respectively. Room temperature mobilities were also measured and are reported elsewhere.[11] The layer compositions were estimated from 5°K photoluminescence measurements. Although a SIMS analysis on a test layer indicated a 12% increase in x in going from the surface to the substrate interface, we assumed for simplicity that x was constant and equal to the value measured by p.l. The layer thicknesses were measured by cleave and stain, and are listed along with the p.l. data in Table A. The last column lists x as estimated from theoretical solidus data for the Ga-Al-As system[11,12], and shows good agreement with the experimental values.

III. ANALYSIS

A. Analysis Technique

The data was analyzed by computer. For each pair of values of x and T, the following calculations were performed. (1) The various physical parameters, namely the effective electronic mass (m*), the static and optical dielectric constants (K_s, K_o), the longitudinal and transverse elastic constants (c_ℓ, c_t), the deformation potential (Ξ_c), the piezoelectric constant (h_{14}) and the longitudinal optical phonon energy (LOPE, $h\omega_\ell$), were estimated, and used to calculate the three lattice scattering times as functions of ε.

(2) A subroutine "MOBILITY" was used for calculating μ_H and μ_D, given x, T, B, EBSQ (test value of E_B^2) and NS (test value of N_S).

(3) For a series of test values of E_B^2, the parameter NS was adjusted to generate a μ_H equal to the measured value. The corresponding drift mobility μ_D and Hall factor $r_H = \mu_H/\mu_D$ were also calculated.

(4) The free carrier density was calculated from[13]

$$N = \frac{r_H Q_H}{d-d_{sc}} \tag{6}$$

where d is the layer thickness and d_{sc} is the sum thickness of the surface and interface depletion regions.[13] The surface and interface barrier heights used for estimating d_{sc} were, respectively[13]

$$SBH = (0.6 + 0.8x)\ eV \tag{7}$$

$$IBH = (0.75 + 1.1x)\ eV \tag{8}$$

The variation of SBH with x was estimated from reference (14), while for IBH it was assumed equal to the variation of ΔE_c with x.[15]

(5) From the values of NS and N calculated in the previous two steps, ND + NA and hence ND and NA were calculated using Eqs. (24) and (25).*

(6) Thus for each test value of EBSQ, values of NA were generated at each temperature. Since in n-type material,

---

*NS, ND, NA, N and EBSQ represent test values of the physical parameters N_S, N_D^+, N_A, n and E_B^2.

the ionized acceptor density is temperature independent, the constancy of NA with T was used as the criterion for selecting E_B^2 from the series of test values of EBSQ. The corresponding values of NA, ND and N were taken to represent N_A, N_D and n.*

(7) To summarize, the program took as its input the values of x, d, B, sets of (T, μ_H, Q_H), and test values of E_B^2, and printed out values of NA, ND and N vs T for each test value of E_B^2.

B. Estimation of Parameters

The relative effective mass (m^*/m_o) for electrons was assumed to be .067 in GaAs[16] and .014 in AlAs[17] at temperatures below 110°K. Its variation with x was calculated from[18]

$$\left(\frac{m^*}{m_o}\right) = \left(\frac{x}{.14} + \frac{1-x}{.067}\right)^{-1} \qquad (9)$$

The static and optical dielectric constants for $Ga_{1-x}Al_xAs$, denoted by K_s^x and K_o^x respectively, were calculated from the expression[18]

$$\frac{K^x-1}{K^x+2} = \left(\frac{K^o-1}{K^o+2}\right)(1-x) + \left(\frac{K^1-1}{K^1+2}\right)x \qquad (10)$$

where K^o and K^1 refer to values for x = 0 and 1 respectively. K_s^o was obtained as[19]

$$K_s^o = 12.91\ \{1 - (300-T) \times 10^{-4}\}\ , \qquad (11)$$

while K_o^o, K_s^1, and K_o^1 were assumed to remain proportional to K_s^o at all temperatures, their room temperature values being 10.91, 10.9 and 8.5 respectively[19,20].

---

*See footnote on page 8

According to Keyes[21], the elastic constants of III-V compounds vary only with the lattice parameter a which for $Ga_{1-x}Al_xAs$ is virtually independent of x. The longitudinal and transverse elastic constants c_ℓ and c_t[22] of GaAs were therefore used for (Ga,Al)As, so that[20]

$$c_\ell = 1.444 \times 10^{12} (1-5.4\times10^{-5}T) \text{ dynes/cm}^2 \quad (12)$$

and

$$c_t = .4905 \times 10^{12} \text{ dynes/cm}^2 \quad (13)$$

Also according to Keyes[23], dE_c/dP (where P is the hydrostatic pressure) is the same for all III-V compounds with the zinc blend structure. Since the elastic constants are assumed to be independent of x, it follows that the variation of E_c with strain is also x-independent. The deformation potential of the Γ_c band edge in $Ga_{1-x}Al_xAs$ was therefore assumed constant at 7.0 eV, the value determined by Wolfe et al[22] for GaAs.

Estimation of the piezoelectric constant h_{14}(V/cm) was based on the assumptions that (i) the dimensionless product $\varepsilon_s h_{14}/e_{14}$ (ε_s = static permitivity) is constant for all III-V semiconductors, and (ii) e_{14}, which is the piezoelectric charge per unit strain, varies linearly with x. The first assumption was verified by testing measured values of h_{14} and e_{14} for five direct band III-V compounds[24], for which $\varepsilon_s h_{14}/e_{14}$ was found to be constant within 5%. $h_{14}(x)$ was obtained from

$$h_{14}^x \equiv h_{14}(x) = \frac{xK_s^1 h_{14}^1 + (1-x)\, K_s^o h_{14}^o}{K_s^x} \quad (14)$$

where h_{14}^{o} was assumed to be 1.4×10^{7} V/cm[22], and h_{14}^{1} was obtained as $\approx 1 \times 10^{7}$ V/cm by assuming e_{14}(AlAs) to be .1, the value for e_{14}(GaP), as estimated by Hauser[25].

The temperature variation of the longitudinal optical phonon energy (LOPE, $h\omega_{lo}$) for GaAs was obtained from the consideration that

$$\omega_{lo} \sim (c_l/M)^{1/2}$$

where M is the reduced mass, and that

$$\frac{1}{c_l}\frac{dc_l}{dT} \approx -5.4 \times 10^{-5} ,$$

so that

$$\frac{1}{\omega_{lo}}\frac{d\omega_{lo}}{dT} \approx -2.7 \times 10^{-5} . \qquad (15)$$

The variation of $h\omega_{lo}$ with x for the GaAs-like and the AlAs-like phonon branches, denoted by LOPE(1) and LOPE(2) respectively, in the range $x < .3$, was obtained from the data of Ilegems[20,26]. The base temperature values were obtained from references (22) and (26) respectively, to give the expressions

$$\text{LOPE(1)} = 36.465\,[1 + 2.7\times10^{-5}\,(77-T)] - .625x \text{ meV} \qquad (16)$$

and

$$\text{LOPE(2)} = 44.7\,[1 + 2.7\times10^{-5}(300-T)] + 15.5x^{2} \text{ meV} \qquad (17)$$

C. Calculation of Relaxation Times and Mobilities

The expressions for the deformation potential and the piezoelectric scattering relaxation times were taken

from reference (22):

$$\tau_{DP}(\varepsilon)^{-1} = 4.167\text{x}10^{19}\ \Xi_c^2\ c_\ell^{-1}\ (m^*/m_o)^{-3/2}\ T^{3/2}\varepsilon^{1/2}\text{sec}^{-1} \tag{18}$$

$$\tau_{PE}(\varepsilon)^{-1} = 1.0524\text{x}10^{7} h_{14}^2 [\frac{4}{c_t} + \frac{3}{c_\ell}](\frac{m^*}{m})^{1/2} T^{1/2}\varepsilon^{-1/2}\text{sec}^{-1} \tag{19}$$

Polar optical scattering for the binary compounds was represented by a time constant[18]

$$\tau_{PO}(\varepsilon)^{-1} = \tau_{PO}^{o\ -1}\ (\frac{1}{\sqrt{\varepsilon}} + \frac{e^z}{\sqrt{\varepsilon - z}}) \tag{20}$$

where $z = (h\omega_\ell/kT)$, and the second term is considered for $\varepsilon > z$ only. τ_{PO}^o was calculated by obtaining an expression for μ_{PO} in terms of τ_{PO}^o based on Eq. (20), and equating it to the value of μ_{PO} obtained from[27]

$$\mu_{PO}(\text{cm}^2/\text{Vsec}) = \frac{.2357}{[h\omega_\ell(\text{eV})]^{1/2}} \frac{(\frac{1}{K_o^x} - \frac{1}{K_s^x})}{(m^*/m_o)^{3/2}} \frac{\chi(z)}{z^{1/2}} (e^z - 1) \tag{21}$$

where $\chi(z)$ can be approximated by $3\sqrt{\pi z}/8$ for $z > 5$[27], a condition that is valid for GaAs below 85°K.

The presence of two optical phonon branches in $Ga_{1-x}A\ell_xAs$ was treated by assuming that the densities of GaAs-like and AℓAs-like phonons are proportional to (1-x) and x respectively. Thus polar optical scattering in $Ga_{1-x}A\ell_xAs$ was represented as

$$\tau_{PO}(\varepsilon)^{-1} = \frac{1-x}{\tau_{PO}^{o1}} \left[\frac{1}{\sqrt{\varepsilon}} + \frac{e^{z_1}}{\sqrt{\varepsilon - z_1}}\right] + \frac{x}{\tau_{PO}^{o2}} \left[\frac{1}{\sqrt{\varepsilon}} + \frac{e^{z_2}}{\sqrt{\varepsilon - z_2}}\right], \tag{22}$$

where $z_1 \equiv \text{LOPE}(1)/kT$, $z_2 = \text{LOPE}(2)/kT$, and τ_{PO}^{o1} and τ_{PO}^{o2} were calculated from Eqs. (20) and (21), using parametric values for the GaAs-like and the AℓAs-like branches respectively.

Ionized impurity scattering was represented by a relaxation time[22]

$$\tau_{II}(\varepsilon) = 0.41417\ K_s^2\ T^{3/2}(m^*/m)^{1/2} N_S^{-1}\ \varepsilon^{3/2} \tag{23}$$

where

$$N_S = (N_D^+ + N_A^-)\ \bar{g} \tag{24}$$

and

$$\bar{g} = \ell n\ \frac{1.297 \times 10^{14}\ K_s (m^*/m) T^2}{n} - 1, \tag{25}$$

this approximate approach being reasonably valid so long as $\bar{g} > 1$ or 2.

Finally, Eq. (2) was used to represent the alloy-like scattering.

The energy dependent inverse relaxation times of Eqs. (2), (18), (19), (22) and (23) were summed to give the net inverse relaxation time $1/\tau(\varepsilon)$[22], and the drift mobility μ_d was calculated numerically as

$$\mu_d = \frac{q}{m^*}\ \overline{\tau(\varepsilon)} = \frac{q}{m^*}\ \frac{\int_o^\infty \varepsilon^{3/2} \tau(\varepsilon) e^{-\varepsilon} d\varepsilon}{\int_o^\infty \varepsilon^{3/2}\ e^{-\varepsilon} d\varepsilon} \tag{26}$$

The Hall factor r_H was calculated as

$$r_H = (T_2/\omega_o)/(T_1^2 + T_2^2) \tag{27}$$

where

$$T_1 = \overline{\tau(\varepsilon)/(1 + \omega_o^2 \tau(\varepsilon)^2} \tag{28}$$

and

$$T_2 = \overline{\omega_o \tau(\varepsilon)^2 / (1+\omega_o^2 \tau(\varepsilon)^2)} \qquad (29)$$

and

$\omega_o = \frac{qB}{m^*}$ is the cyclotron frequency.

In Eqs. (28) and (29), the bar represents the energy weighted average over a Boltzmann distribution, as expanded in Eq. (26) for $\overline{\tau(\varepsilon)}$.

Thus, given x, T, B, N_S and ΔE^2, the Hall mobility could be calculated as $r_H \mu_D$ and compared with the experimental value.

D. Data Fitting Techniques

The computer program was first tested on the Hall data of the GaAs sample to see if the values of NA generated were temperature independent. NA was found to increase monatonically with temperature from 4.5×10^{14} cm^{-3} at 25°K to 8.3×10^{14} cm^{-3} at 110°K, indicating that the extent of lattice and/or alloy-like scattering was being underrepresented. In our attempts to make NA constant, we studied the effect of varying several parameters. An excellent data-fit below 55°K could be obtained by including a small amount of space charge scattering (by taking x = .0001 and $E_B^2 = 9.1$ eV^2 in Eq. (2), equivalent to $N_s Q = 377$ cm^{-1}), or comparably by using $\Xi_c = 8.3$ eV instead of 7.0 eV. To fit the data in the 55°K - 110°K range, we had to reduce the polar optical relaxation time $\tau_{PO}(\varepsilon)$ by a factor ZZZ = 0.65. Although

this adjustment looked rather arbitrary, it seemed to be the only one that reduced NA sufficiently at higher temperatures to make it (NA) temperature independent, while not affecting it (NA) for $T < 55^{o}K$.

To fit the $Ga_{1-x}A\ell_{x}As$ data, it seemed appropriate to keep Ξ_c constant at 7.0 eV and adjust EBSQ, since EBSQ was a variable parameter anyway. Also, alloy-like scattering was expected to dominate over both D.P. and P.E. scattering in the temperature range studied, for $x \gtrsim 0.05$ (see Discussion). Hence the effect on NA of adjusting Ξ_c or h_{14} would be relatively small compared to the effect of adjusting EBSQ. Thus EBSQ was adjusted to fit the data for $T \lesssim 55^{o}K$. Then the empirically established procedure of adjusting the factor ZZZ was utilized to equalize NA at the higher temperatures.

IV. RESULTS AND DISCUSSION

A. Results

The values of EBSQ and ZZZ that gave the best data fit or the near-best fit for the various samples are listed in Table B, along with the values of NA generated. The quality of data fits, rated excellent, good, fair or poor, is also listed. Some values of E_B^2 differ from the corresponding EBSQ by .01 because equally good "best" fits were obtained for two adjacent values of EBSQ (differing by .02), one of which is listed. The range of E_B^2 indicates the range of EBSQ values for which comparable constancy was obtained for NA. For the GaAs sample F-25, a small but finite value of x (= .0001) was used to allow the inclusion of space

charge scattering. The data for sample F-11 was not analysed.

The values of E_B^2 obtained ranged from .13 eV^2 to .26 eV^2, corresponding to E_B = .36 eV to .51 eV, the average being E_B = .44 eV. Fig. 3 shows the equivalent values of NsQ plotted against x, if the alloy-like scattering is interpreted as consisting of only space charge scattering. While the data is insufficient, the extent of alloy-like scattering seems to be lower in type $B^{(11)}$ (odd numbered) than in type-A (even numbered) samples. The possible significance of this is discussed in Section IV.C.

In addition, the compensation ratio was measured to be about 2 for most of the samples, as shown in Table B.

B. Sources of Error

The results of this experimental analysis are subject to uncertainties and errors, both random and systematic, from a variety of sources, namely data measurement, parameter estimation, approximations made in the mathematial formulation, and the data fitting technique for which no a priori justification could be provided. For the apparatus used, we would estimate the uncertainties in B, μ_H, Q_H, T, and d to be about $\pm$3%, $\pm$4%, $\pm$10%, $\pm$5% and $\pm$ 0.75μ respectively, and the uncertainty in x for most samples to be $\pm$ .01.

The 'formulation' errors arise from the various approximations made. For instance, the assumption $1/\tau = \sum_i 1/\tau_i$ is not strictly accurate[22]. The non-degenerate (Boltzman's) approximation is largely valid for the high purity samples

but is in error by a few percent, specially at the lower temperatures. The energy averaging of the screening factor g in Eqs. (24) and (25) instead of using the energy dependent $g^{(22)}$ can cause significant error, specially at higher doping and low temperatures. Again, for n below 1×10^{15}, this error is small at 25°K. Finally the $T^{-1/2}$ dependence of space charge scattering assumed as mentioned earlier, might not be correct.

The seemingly arbitrary need to reduce $\tau_{PO}(\varepsilon)$ of Eq. (22) by a factor ZZZ ($\simeq .6$) to fit the data could be a result of inaccuracies in Eq. (21) for μ_{PO}. The solution of Boltzmann's equation for polar optical scattering is complex, and has led to a variety of different expressions.[27,30,31] The term $\chi(z)$ in particular, which we have approximated by $3\sqrt{\pi z}/8$, can be in significant error by a temperature dependent factor which is compensated in our analysis by ZZZ. Compounding this formulation error is the high sensitivity of the calculated value of μ_{PO} to some of its parameters. For instance, a 1% error in estimating either K_s or K_o would lead to a 7% error in μ_{PO}, as would a 1% error in z at 60°K. Finally, using a relaxation time approximation for μ_{PO} itself could have caused some error which required compensation.

Finally, to illustrate the effects of errors in estimating the various physical parameters, we select sample F-17 (x = .11). Fig. 4 shows the calculated values of μ_{PE}, μ_{DP}, μ_{PO}, μ_{AL} and μ_{II} plotted against T. The

mobilities correspond to the estimated or measured values of the relevant parameter for sample F-17, except for μ_{PO}, which is shown for ZZZ = 1. For calculating μ_{II}, we assumed $N_D = 3N_A$.

It is seen that between 25°K and 100°K, ionized impurity scattering and alloy-like scattering dominate over the others, which implies that the effect of varying μ_{PE}, μ_{DP}, and μ_{PO} on μ_{total} is small, especially in the lower half of the temperature range. For example a 10% error in estimating h_{14} would cause only a 1% error in E_B. However, for samples with lower x, μ_{AL} is higher and the value of E_B is more susceptible to errors in the estimation of lattice scattering. For temperatures below ~60°K, ionized impurity scattering dominates, so that the values of NA generated are more accurate. At higher temperatures, $N_D + N_A$ is estimated from a smaller component of the total scattering, and is therefore subject to larger systematic errors, which might also contribute to the ZZZ factor.

C. Discussion

Both Kaneko et al.[9] and Stringfellow[10] report a good theoretical fit to their μ vs T data by assuming the space charge scattering parameter N_sQ to vary as

$$N_sQ = 5x10^3 + 6.3x10^5x \quad . \tag{30}$$

By substituting Eq. (30) in Eq. (4) and comparing with Eq. (2) at x = .1, .2 and .3, it is seen that space charge scattering described by Eq. (30) is equivalent to alloy-like scattering

with $E_B^2 = 1.64\ eV^2$. In constrast, we obtain values of E_B^2 from .13 to .26 eV^2, or equivalently

$$N_s Q \approx 8.6 \times 10^4 x \quad . \tag{31}$$

The samples from references (9) and (10) were doped in the range of $10^{17}\ cm^{-3}$, about two orders of magnitude higher than our samples. Given this limited information, some correlation is seen to exist between the extent of space charge scattering and the sample purity. Even among our samples, we measure lower values of E_B^2 for the type B samples compared with the less pure type A samples, although layer F-19 (x = .154, NsQ = 16600) violates this rule.

We find it difficult to draw conclusions about the extent of alloy scattering in our samples, except that ΔE is definitely lower than $\Delta E_g = .7$ eV. The fact that the measured values of E_B^2 differ by as much as 2:1 suggests the presence of some space charge contribution to E_B^2, though we cannot rule out the possibility that this variation results mainly from measurement and analysis errors. If Ferry's[5] estimation that $\Delta E = .12$ eV is indeed correct, then the alloy scattering contribution to the measured value of E_B^2 will be negligible. On the other hand, if the value of ΔE predicted by Harrison and Hauser's[3] model, (55eV), is reasonably true, then alloy scattering will contribute a major part of E_B^2.

D. Summary

Hall mobilities of high purity LPE $Ga_{1-x}A\ell_xAs$ layers were measured as a function of temperature in the range ($0 \leq x < .2$). The various physical parameters that are relevant to electron scattering were estimated for $Ga_{1-x}A\ell_xAs$, using the best extrapolation techniques available to us. A computer program was used to generate Hall mobilities as a function of the independent experimental and sample parameters, namely, x, T, B, E_B and N_S, and to adjust N_S for test values of E_B to obtain agreement with experiment. From N_S and the carrier concentration, the acceptor density N_A was calculated, and its constancy with temperature was used as the criterion for selecting E_B from its test values. The alloy-like scattering parameter E_B was measured to lie between .36 eV and .51 eV, the average value being .44 eV. The extent of alloy-like scattering in our samples was thus an order of magnitude lower than in samples of references (9) and (10). No definite conclusions could be reached about the value of ΔE, the depth of the random potential well in $Ga_{1-x}A\ell_xAs$, except for placing an upper limit of $\simeq .5$ eV on its value.

ACKNOWLEDGEMENTS

We would like to thank Dr. Ron Nelson of Bell Labs for taking the photoluminescence measurements. This work was supported by the Office of Naval Research, under contract # N00014-75-C-0739.

REFERENCES

1. H. Brooks, unpublished.

2. J.J. Tietjen and L.R. Weisberg, Appl. Phys. Lett., 7, 261, (1965).

3. J.W. Harrison and J.R. Hauser, Phys. Rev., B13, 5347, (1976).

4. Makowski and M. Glicksman, J. Phys. Chem. Sol. 34, 487, (1973).

5. D.K. Ferry, Phys. Rev., B17, 912, (1978).

6. L.R. Weisberg, J. Appl. Phys., 33, 1817, (1962).

7. E.M. Conwell and M.O. Vassel, Phys. Rev., 166, 797 (1968).

8. T. Katoda and T. Sugano, J. Electrochem Soc., 121, 1065, (1964).

9. K. Kaneko, M. Ayabe and N. Watanabe, Proc. 6th Intn'l. Symp. on GaAs and Related Compounds, Edinburgh, 216, (1976).

10. G. Stringfellow,"Electron Mobility in $A\ell_xGa_{1-x}As$", J. Appl. Phys., to be published.

11. A. Chandra and L.F. Eastman, "The Liquid Phase Epitaxial Growth of High Purity $Ga_{1-x}A\ell_xAs$", submitted to J. Electrochem. Soc.

12. Y.D. Shen, communicated by G.L. Pearson.

13. A. Chandra, C.E.C.Wood, D. Woodard, L.F. Eastman, "Surface and Interface Depletion Corrections for Carrier Density Determination by Hall Measurements", Solid State Electronics, to be published.

14. G.L. Pearson, private communication.

15. R. Dingle, W. Wiegmann and C.H. Henry, Phys. Lett., 33, 827, (1974).

16. D.E. Aspnes, Proc. 6th Intn'l. Symp. on GaAs and Related Compounds, St. Louis, 110, (1976).

17. D.J. Stukel and R.N. Euwema, Phys. Rev., 188, 1193, (1969).

18. J.W. Harrison and J.R. Hauser, J. Appl. Phys., 47, 292, (1976).

19. D.L. Rode, Semiconductors and Semimetals (Editors: Willardson and Beer), 10, 1.

20. M. Neuberger, "Handbood of Electronic Materials," Vol. 2. III-V Semiconducting Compounds, Publ. IFI/Plenum, New York, 1971.

21. R.W. Keyes, J. Appl. Phys., 33, 3371, (1962).

22. C.W. Wolfe, G.E. Stillman and W.T. Lindley, J. Appl. Phys., 41, 3088, (1970). This paper lists other relevant references.

23. R. Keyes, Semiconductors and Semimetals, (Editors: Willardson and Beer), 4, 327.

24. G. Arlt and P. Quadflieg, Phys. Stat. Sol. 25, 323, (1968).

25. J. Hauser, Private Communication.

26. M. Ilegems, Ph.D. Dissertation, Stanford University, (1979).

27. R.L. Petritz and W.W. Scanlon, Phys. Rev., 97, 1620, (1955).

28. J.P. McKelvey, Solid State and Semiconductor Physics, Harper and Row (New York, 1966), John Weatherhill, Inc. Tokyo), Section 9.8.

29. B.R. Nag, Theory of Electrical Transport in Semiconductors, Int'l Series in the Science of Solid State: V3, Pergamon Press, (1973).

30. A. Fortini, D. Dignet, and J. Lugand, J. Appl. Phys., 41, 3121, (1970).

31. D.J. Howarth and E.H. Sondheimer, Proc. Roy. Soc., (London) A219, 53, (1953).

Table A

Thickness and Composition Data for the

$Ga_{1-x}Al_xAs$ ($0 \leq x < .18$) Studied

Sample #	Thickness (microns)	Photoluminescence (5^oK) peak energy (eV)	x, from p.ℓ. %	x from thermodynamics %
F-25	14.0			0
F-10	11.1	1.545	2.0	2.1
F-11	11.1	1.541	1.75	1.75
F-12	12.0	1.581	4.6	5.1
F-13	13.9	1.577	4.2	4.3
F-14	11.4	1.632	8.2	8.8
F-15	13.0	1.625	7.8	7.7
F-16	11.1	1.682	11.8	12.6
F-17	10.3	1.670	11.0	11.3
F-18	9.3	1.744	17.7	17.1
F-19	9.5	1.726	15.4	15.6

Table B

Values of NA (...x$10^{14}$$cm^{-3}$) Generated for Best Fit

(or near best fit) of Data

Sample #F		25	10	11	12	13	14	15	16	17	18	19
x(%) used		0.01	2.0	1.75	4.6	4.2	8.2	7.8	11.8	11.0	17.7	15.5
Best fit (or near best fit) values	EBSQ	9.1	0.20		.18	.12	.20	.12	.25	.16	.21	.27
	ZZZ	0.65	0.65		.66	.68	.6	.65	.5	.55	.55	.55
Temp(K)												
25								3.40	4.95	2.42		3.70
30		4.22	4.63			3.76	4.20	3.60	5.01	2.48		3.54
35		4.31	4.62			3.70	4.01	3.50		2.21		3.43
40		4.28	4.33		3.92	3.51	3.96	3.49	4.48	2.17	6.74	3.37
45		4.30	4.29		3.84	3.32	4.03	3.45	4.45	2.21	6.64	3.41
50		4.27	4.27		3.77	3.33	4.05	3.51	4.44	2.25		
55		4.28	4.30		3.77	3.37	4.16	3.61	4.44	2.30		3.44
60			4.35		3.74	3.37	4.19	3.68	4.48	2.33	6.52	
65		4.35	4.39		3.80	3.43	4.36	3.83	4.55	2.35	6.82	3.68
70			4.38		3.79	3.42	4.42	3.84	4.51	2.32	7.03	
75		4.37	4.56		3.79		4.53	3.88	5.00	2.24	6.96	3.83
80			4.30		3.78	3.54	4.54	3.90	4.62		7.33	3.66
85		4.34	4.21		3.77		4.58	3.62	4.90		7.50	3.70
90			4.20		3.65	3.47	4.52	3.54	4.72		7.64	3.75
95		4.35	4.08		3.51	3.34	4.55	3.34	4.44			3.76
100		4.31	4.36		3.51	3.27	4.48	3.26	4.24			3.78
110		4.38	3.85		3.24		4.53	3.02	3.77			4.06
Comments		Exc	Good		Exc	Good	Fair	Poor	Fair	Good	Poor	Fair
$E_{B_2}^2$ (eV^2)			.21 ±.03		.18 ±.02	.13 ±.02	.20 ±.03	.14 ±.02	.25 ±.02	.16 ±.02	.21 ±.03	.26 ±.02
E_B(eV)			.46		.42	.36	.45	.37	.50	.40	.46	.51
n_{75}(x$10^{14}$$cm^{-3}$)		1.1	4.3		7.4	5.0	8.5	5.9	9.0	4.8	---	2.9
N_A(x$10^{14}$$cm^{-3}$)		4.3	4.2		3.8 ±0.6	3.1 ±0.3	4.3 ±0.3	3.1 ±0.9	4.5 ±0.4	2.3 ±0.3	--- ---	4.4 ±0.5
Compensation Ratio($\frac{2N_A}{n}$ +1)		9	3.0		2.0	2.2	2.0	2.1	2.0	2.0	-2	4.0

NOT ANALYZED

FIGURE CAPTIONS

1. Hall mobility vs temperature data for $Ga_{1-x}A\ell_xAs$ Samples.
2. Hall carrier density per unit area (Q_H) vs temperature data for $Ga_{1-x}A\ell_xAs$ samples. The discontinuities were caused by a 'set-up' error.
3. Space charge parameter NsQ (assuming all alloy-like scattering to be due to space charge scattering) plotted against x. The vertical lines are error bars estimated from the uncertainty in measuring E_B^2.
4. The calculated temperature variation of the various mobility components for representative sample F-17 (x = .11). Values of the physical parameters used in the calculations are: Ξ_c = 7.0 eV, $h_{14} = 1.4 \times 10^7 V \cdot cm^{-1}$, $E_B^2 = .15\ eV^2$, $N_D + N_A = 1 \times 10^{15}\ cm^{-3}$ and $N_D = 3N_A$. For the μ_{PO} curve, ZZZ was assumed to be unity. The curve marked μ represents the experimental Hall mobility.

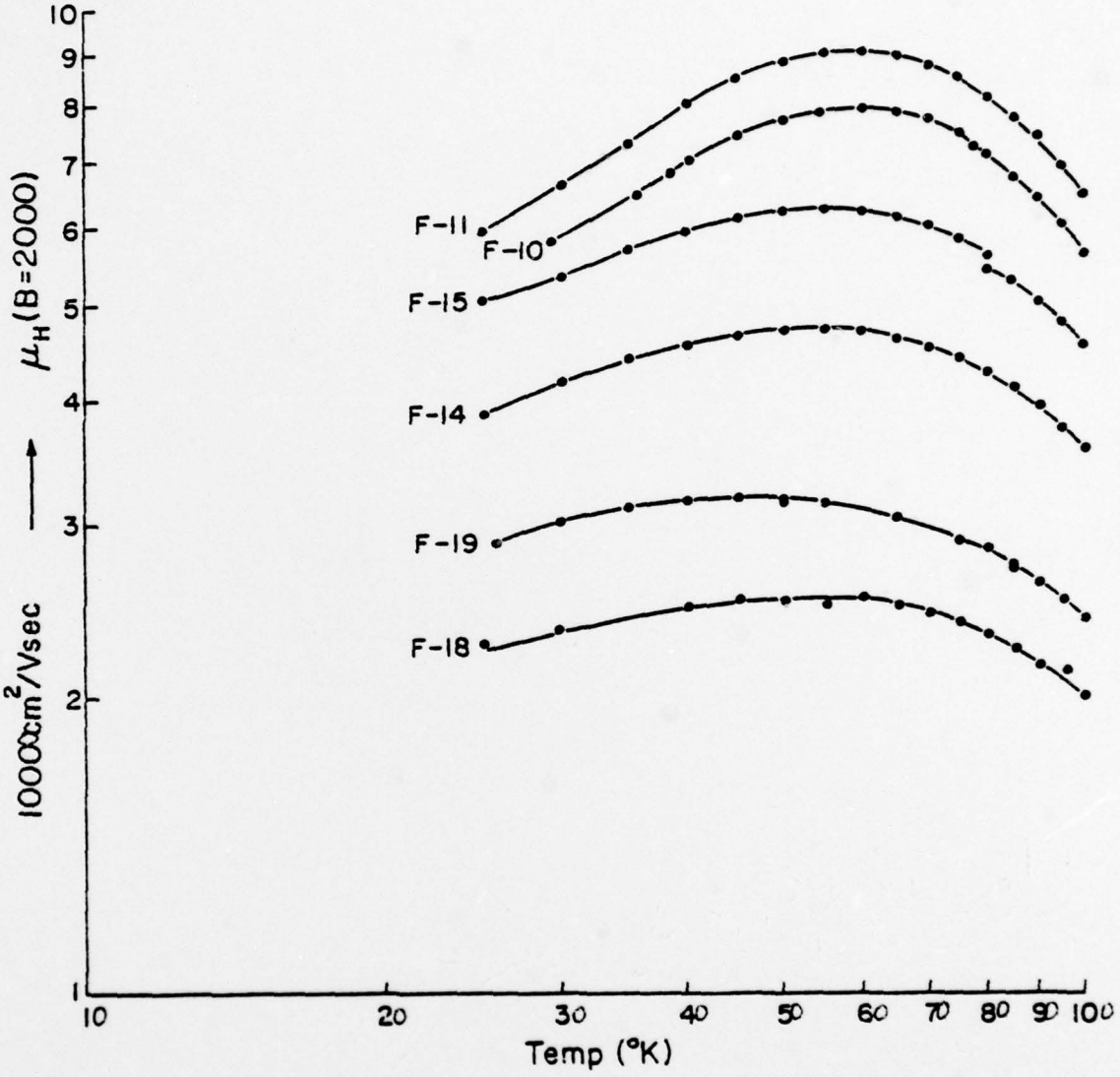
10
9
8
7
6
5
4
3
2
1
μ_H(B=2000)
10000cm^2/Vsec
F-11
F-10
F-15
F-14
F-19
F-18
10
20
30
40
50
60
70
80
90
100
Temp (°K)

Fig 1(a)

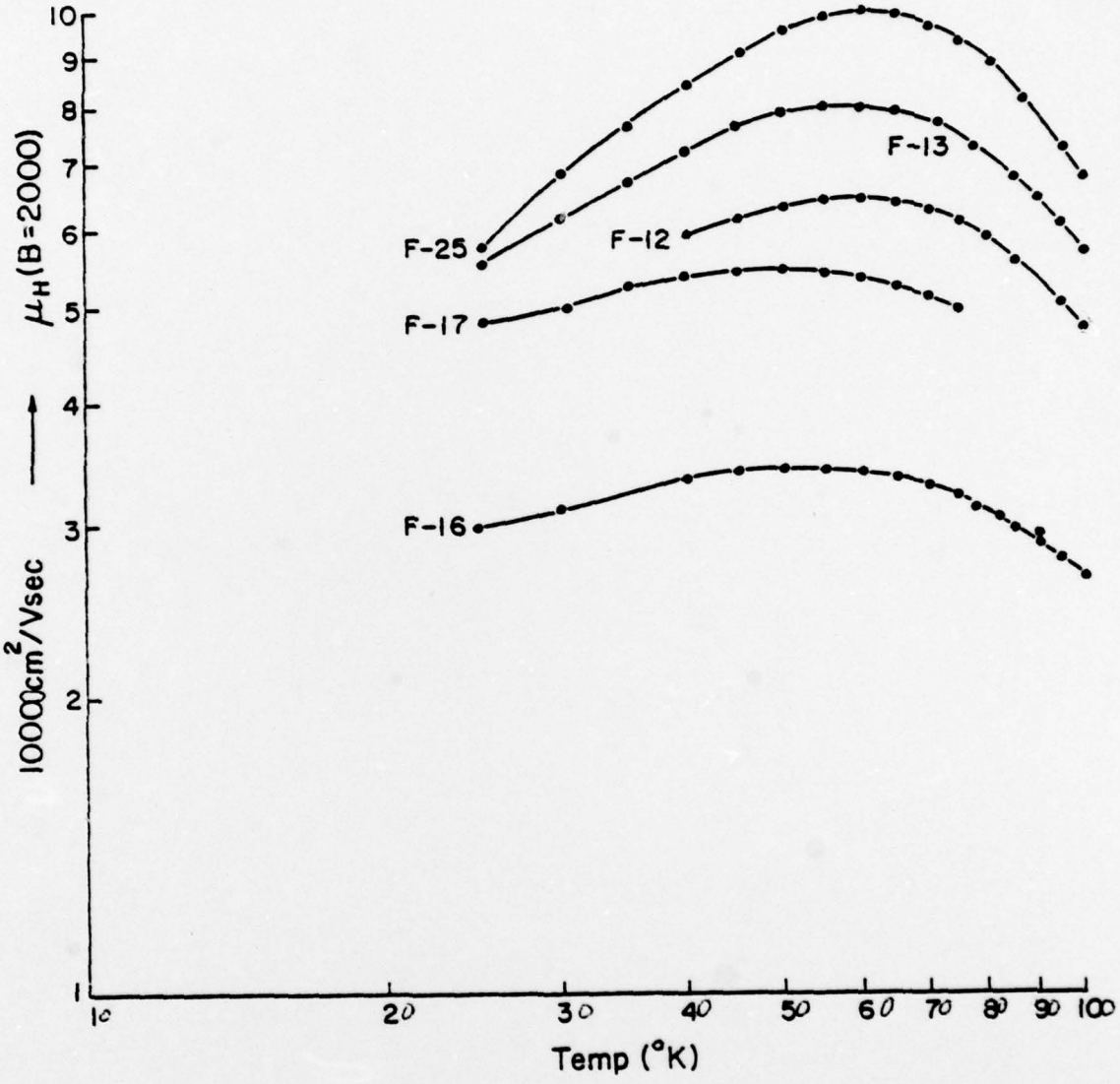
10
9
8
7
6
5
4
3
2
1
μ_H(B=2000)
10000cm²/Vsec
F-25
F-13
F-12
F-17
F-16
10
20
30
40
50
60
70
80
90
100
Temp (°K)

Fig 1(b)

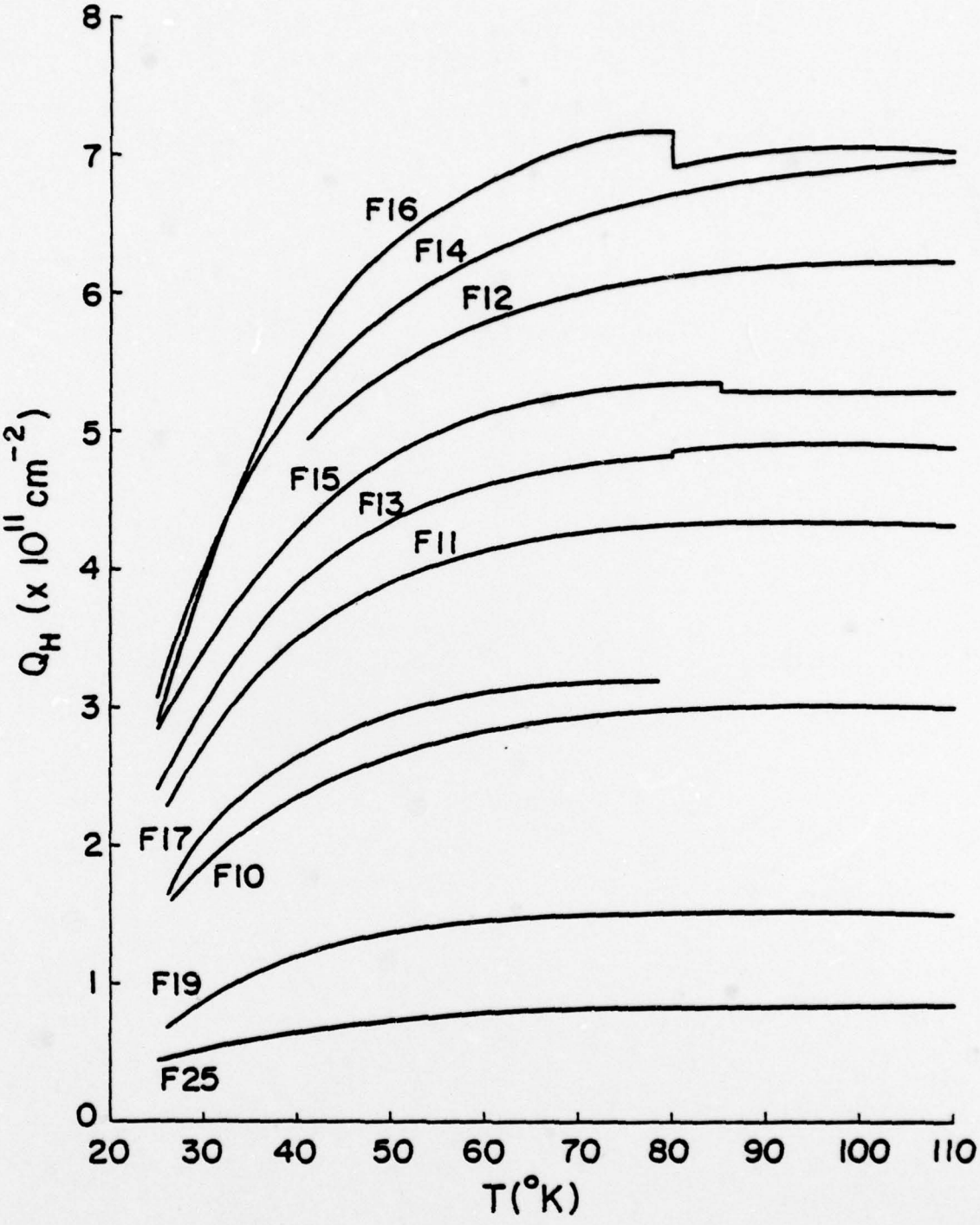
8
7
6
5
4
3
2
1
0
Q_H (x 10^{11} cm^{-2})
F16
F14
F12
F15
F13
F11
F17
F10
F19
F25
20
30
40
50
60
70
80
90
100
110
T(°K)

Fig 2.

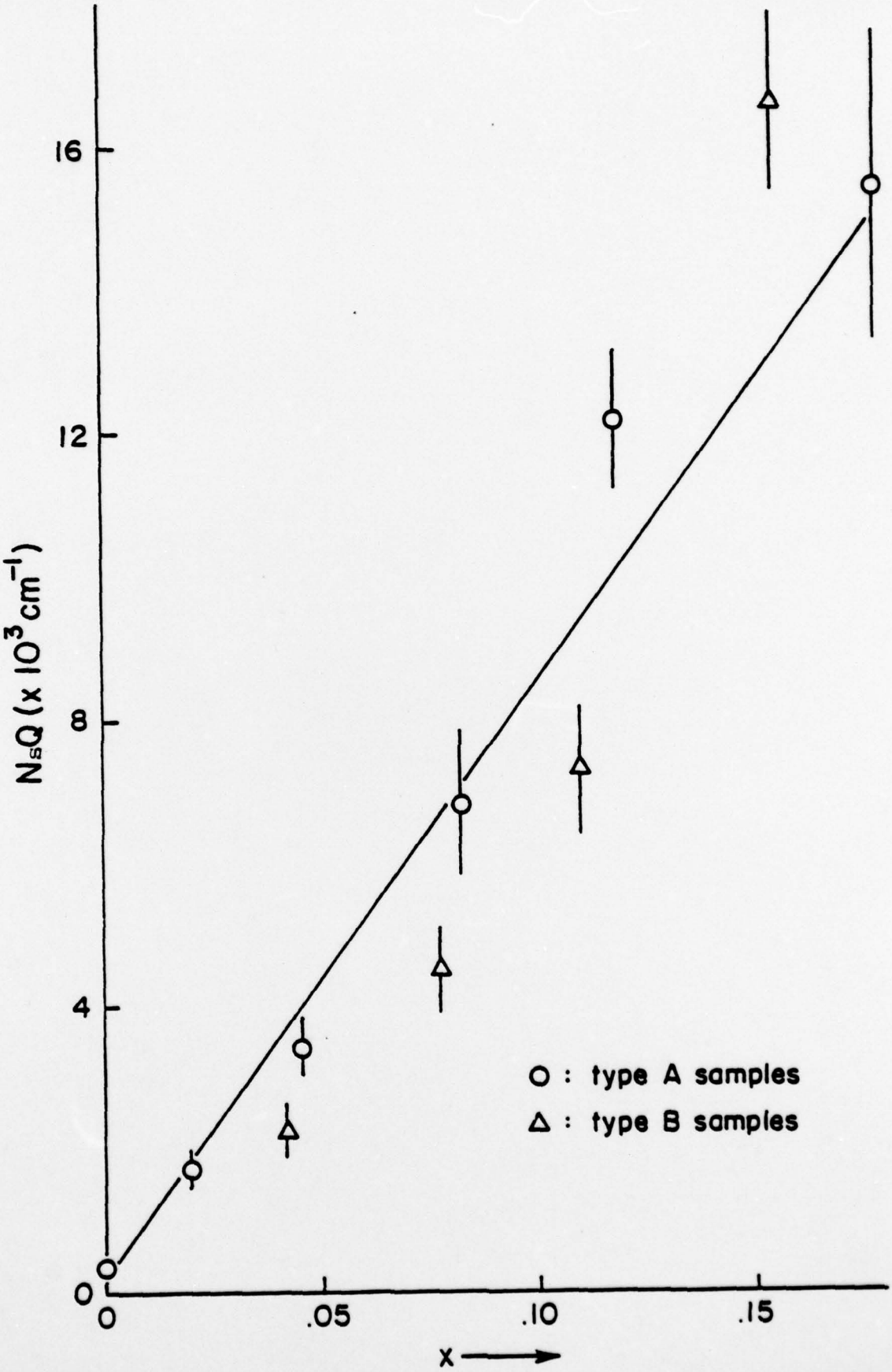

Fig 3

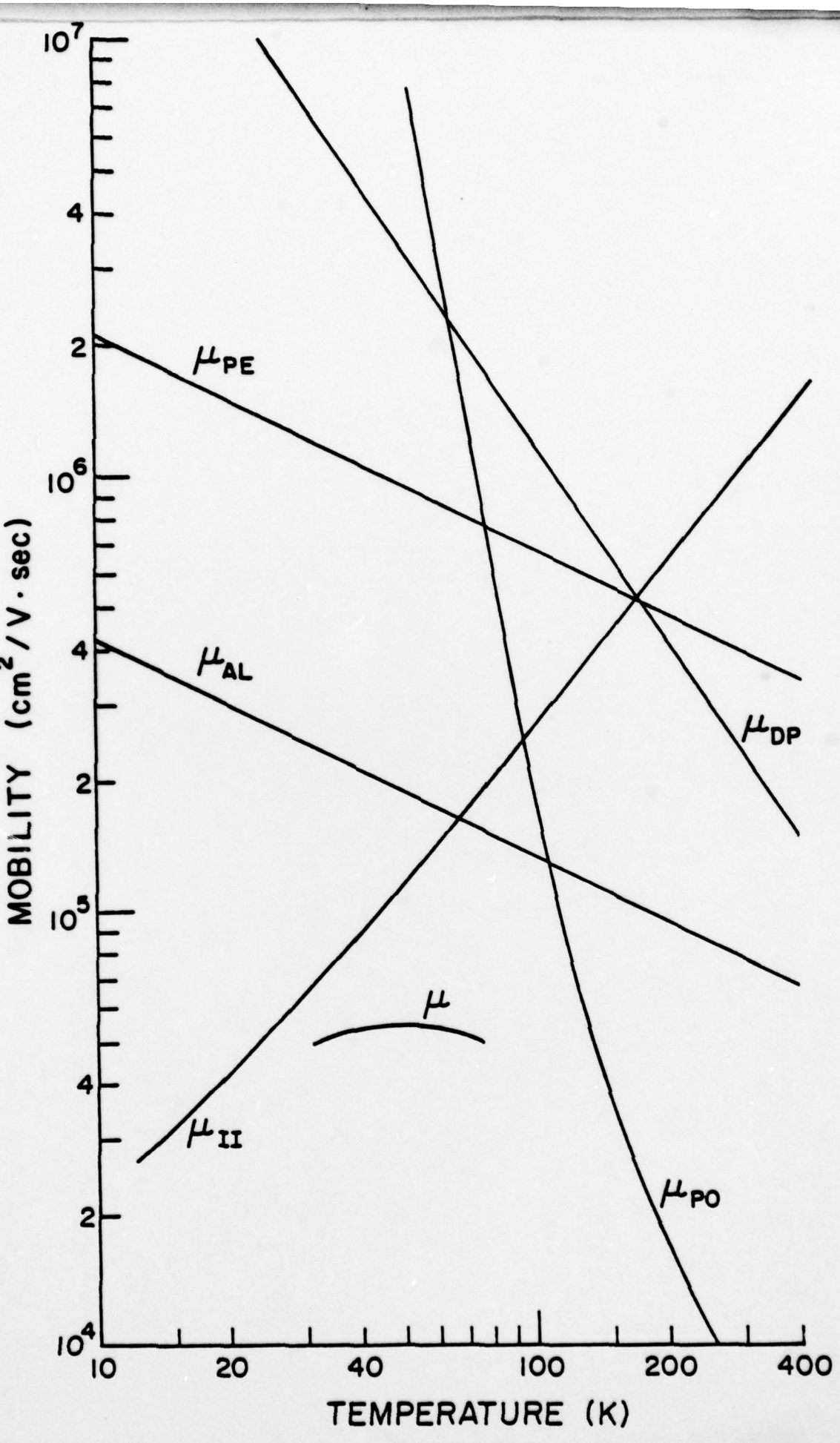
MOBILITY (cm²/V·sec)
10⁷
4
2
10⁶
4
2
10⁵
4
2
10⁴
μPE
μAL
μDP
μ
μII
μPO
10
20
40
100
200
400
TEMPERATURE (K)